Aalborg Universitet

Multi-path Cluster characteristics in Indoor Environments at 28 GHz Band

Hanpinitsak, Panawit ; SAITO, Kentaro ; Fan, Wei; Hejselbaek, Johannes; Takada, Junichi; Pedersen, Gert Frølund

[Link to publication from Aalborg University](#)

Multi-path Cluster characteristics in Indoor Environments at 28 GHz Band

Panawit HANPINITSAK[†], Kentaro SAITO[†], Wei FAN[††], Johannes HEJSELBAEK[†††], Jun-ichi

TAKADA[†], and Gert FRØLUND PEDERSEN[††]

† Department of Transdisciplinary Science and Engineering

School of Environment and Society, Tokyo Institute of Technology

S6–4, 2–12–1, O-okayama, Meguro-ku, Tokyo, 152–8550, Japan

†† Department of Electronic Systems, Faculty of Engineering and Science

Aalborg University, DK-9220, Aalborg, Denmark

††† Nokia Bell Labs, DK-9220, Aalborg, Denmark

E-mail: †{hanpinitsak@ap.ide.titech.ac.jp,saitouken@tse.ens.titech.ac.jp,takada@ide.titech.ac.jp},

††{wfa@es.aau.dk,gfp@es.aau.dk}, † † †{joh@ieee.org}

Abstract　This paper presents the characteristics of multi-path clusters in indoor hall and classroom environments at 28 GHz Band. Firstly, space alternating generalized expectation maximization (SAGE) was used to estimate the multi-path components (MPCs) from the measurement data. Secondly, scattering point-based KPowerMeans (SPKPM) algorithm was applied to estimate and track the clusters based on the physical object position. Finally, the mean of cluster delay and angular spreads were computed. The results showed that the cluster spreads were mostly small which indicates that the channel is highly directive at 28 GHz band.

Key words　Indoor environments, Millimeter wave propagation, clustering

1. Introduction

Due to the increase of high data rate applications such as 4K and 8K videos, virtual reality (VR), and augmented reality (AR), the 5th generation (5G) wireless system using millimeter wave bands has been considered as a key to accommodate the data traffic due to large available bandwidth [1,2]. Additionally, due to the small wavelength, the massive number of antennas can be mounted without increasing the physical size of the antenna array to send multiple streams concurrently. Although 60 GHz band has been the most popular because of its priority, 28 GHz band is also one of the potential candidates and thus has been widely examined, especially in the indoor environments. [3–8].

As the surrounding environment has a significant impact on wireless communication performance, the channel model and characterization are needed. The large scale parameters such as path loss, delay spread, angular spread, as well as spatio-temporal characteristics have been analyzed [3–8]. Since the measurements from these works were conducted at dissimilar environments with different interacting objects (IOs), the channel characteristics and results of the channel model may be different [9]. This is because the contribution of each IO has a significant effect on the channel property. Each IO is also comprised of several diffuse and specular multi-path components (MPCs), which forms a geometry-based cluster [10].

Therefore, as insights to improve the channel model, the study, clarification, and understanding of the geometry-based cluster's physical mechanism are extremely important. Thus, several literatures started to study the geometry-based cluster characteristics. For instance, [11] studied cluster power and spread properties at 11 GHz. In [12], the major mechanisms of clusters were analyzed at 70 GHz. At 60 GHz, [13,14] provided the cluster gain and reflection loss, [15] analyzed the cluster through the angular power spectrum, and [16] provided the double-directional and polarization characteristics of clusters. Recently, the frequency dependence of geometry-based clusters' scattering intensities from 3 to 28 GHz in an indoor hall environment was analyzed by the authors [17]. However, to the authors' best knowledge, the physical interpretation of intra-cluster spread characteristics in different indoor environments at 28 GHz band is still very limited.

Thus, in this paper, the clustering results and their delay and angular spreads [18] in hall and classroom environments at 28 GHz band are presented. The clusters were obtained and tracked by using the SIMO scattering point-based KPowerMeans (SPKPM) algorithm [17], which is the extension of the conventional KPowerMeans (KPM) algorithm [19]

and MIMO-based SPKPM algorithm [11,20]. After that, the delay spreads (DSs) and angular spreads (ASs) were calculated from the delay and angle of MPCs in each cluster. The results showed that the spreads in the classroom environment were slightly higher than those of the hall environment due to more objects with rough or complex surface. Nevertheless, the delay and angular spreads were mostly smaller than deg and ns, respectively. This implies that the channel is highly directive with small diffuse components at 28 GHz band.

The rest of the paper is arranged as follows: Section 2 explains the radio channel measurement. In Section 3, the data analysis methods are described. Then, Section 4 presents the clustering and cluster spread results. Finally, in Section 5, the conclusion is provided.

2. Virtual Array Radio Channel Measurement Method

The measurement was conducted by utilizing the virtual uniform circular array (UCA) channel sounding system [21,22]. Fig. 1 illustrates the channel sounding system which contains five parts. The vector network analyzer (VNA) was used to sweep the signal. The reference and test mixers were exploited to down-convert to transmitted and received signals to intermediate frequency (IF) signal. To rotate the antenna at each position, the rotator was used. At each position, the single-input, single-output (SISO) channel transfer function at the i-th Rx location ($\boldsymbol{H}_i$) was computed from the IF signals down converted from both the receiver (Rx) and transmitter (Tx). The single-input, multiple-output (SIMO) channel transfer function of the UCA was then realized after rotating the automatic rotator to every position.

The operation steps of the sounder are as follows: Firstly, the trigger is sent from the rotator so that the VNA make the sweep. After that, the VNA send another trigger to the rotator so that it rotates to the new position. Finally, the rotator sends the trigger to VNA gain to make it sweep. These processes were replicated until the rotator moves to every Rx antenna positions. Therefore, the SISO channel transfer functions were used to create the SIMO channel transfer function by

$$\boldsymbol{H} = [\boldsymbol{H}_0, \boldsymbol{H}_1, ..., \boldsymbol{H}_i, ..., \boldsymbol{H}_{I-1}] \tag{1}$$

where I, $\boldsymbol{H}_i$ are the number of Rx antenna locations, channel transfer function at i-th Rx location, respectively.

3. Data Analysis Methods

3.1 Cluster Calculation Methods

Fig. 2 illustrates the flow chart of the data analysis method. First, the MPC parameters which are angle-of-arrival (AoA), elevation-of-arrival (EoA), and delay time (DT) were estimated from the measured transfer function using space alternating expectation maximization (SAGE) algorithm [23,24] with spherical wave model [25,26]. Then, measurement-based ray tracer (MBRT) [17,27] was exploited to estimate the scattering point position utilizing the MPC parameters and geometric map. The MBRT was able to distinguish the scattering points based on the number of bounces with the objects which are 1. Single bounce (SB), 2. Double bounce (DB), and 3. Triple bounce (TB). After that, the SPKPM was utilized to calculate and track the geometry-based clusters using those scattering points and geometric map [11,17]. It should also be noted that the cluster with a different number of bounces may be combined into one cluster to compensate the ambiguity of the scattering point estimation caused by the resolution limits of the parameter estimation [17]. The details of implementation are provided in [11,17].

3.2 Cluster Spread Calculation Methods

After the geometry-based clusters were obtained from the SPKPM algorithm, the AS and DS of cluster k were calculated by

$$AS_k = \sqrt{\frac{\sum_{l \in \mathcal{C}_k} P_l \cdot (\phi_l - \bar{\phi}_k)^2}{\sum_{l \in \mathcal{C}_k} P_l}} \tag{2}$$

$$DS_k = \sqrt{\frac{\sum_{l \in \mathcal{C}_k} P_l \cdot (\tau_l - \bar{\tau}_k)^2}{\sum_{l \in \mathcal{C}_k} P_l}} \tag{3}$$

where $\mathcal{C}_k$ is the set of MPCs in cluster k. P_l, ϕ_l, and τ_l are the power, AoA and DT of path l. $\bar{\phi}_k$ and $\bar{\tau}_k$ are the AoA and DT centroids of cluster k, which are calculated by the
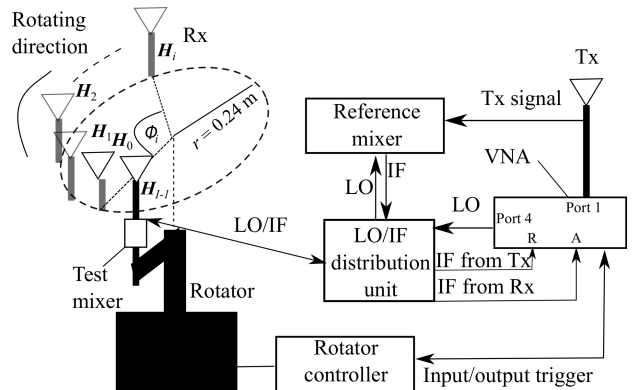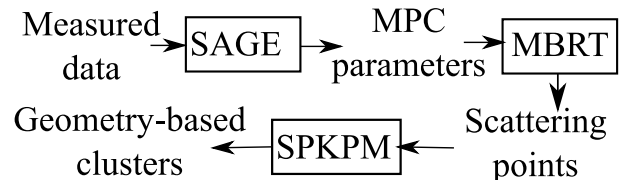

Fig. 1: Virtual UCA system [21,22]

Fig. 2: Flow chart of the data analysis method.

power-weighted mean of AoA and DT

$$\bar{\phi}_k = \frac{\sum_{l \in \mathcal{C}_k} P_l \cdot \phi_l}{\sum_{l \in \mathcal{C}_k} P_l} \tag{4}$$

$$\bar{\tau}_k = \frac{\sum_{l \in \mathcal{C}_k} P_l \cdot \tau_l}{\sum_{l \in \mathcal{C}_k} P_l} \tag{5}$$

After the AS and DS were computed for each cluster at each Tx position, their mean was calculated over all Tx spatial snapshots.

4. Results and Discussion

4.1 Measurement Environments and Specification of the Channel Sounder

We conducted the measurement in hall environment [28], which is a large room with few scattering objects, and classroom [7, 29], which is a smaller room with several smaller objects. Both environments are located in Aalborg University, Aalborg, Denmark. Figs. 3 and 4 depict the floor plan with 20 Tx spatial snapshots in hall environment and classroom environment, respectively. The major objects in the hall environment comprised of plasterboard wall, wood door, concrete pillars, steel tubes, steel elevator, metal studs, and brick wall. In contrast, the classroom environment was covered by plasterboard walls on all six sides. There were black and white boards on the left side wall separated by 21 cm. Windows are covered with a thin metallic layer and are located at the top side. In front of the room, there were blackboard, table, and wood door. 5 illustrates the measurement photographs with antenna array geometry. Rx was a modified biconical antenna [30] mounted on a robot arm which rotates to 360 positions with a 0.24 m radius to mimic the UCA system. Tx was a commercial biconical antenna [31]. Table 1 depicts the measurement setup parameters. In each environment, the measurement was done for 20 spatial Tx snapshots. The Tx was spaced 80 and 100 cm apart for the case of the classroom environment and hall environment, respectively. The height of both Tx and Rx were set to 1.5 m.

4.2 Geometry-Based Clustering Results

Figs. 6 and 7 show the SB, DB, and TB clustering results, as well as the AoA-DT scatter plot at the 2nd snapshot in hall and classroom environments, respectively. The circle, upward pointed triangle and right pointed triangle represent SB, DB, and TB scattering points in Figs. 6 and 7 (d). Scattering points which have the same color belong to the same cluster. The white square denotes the unidentified scattering points where the MBRT algorithm could not find the suitable IO, which could be interpreted as the MPCs scattered from small and insignificant objects. The results showed that

Table 1: Channel sounder specification

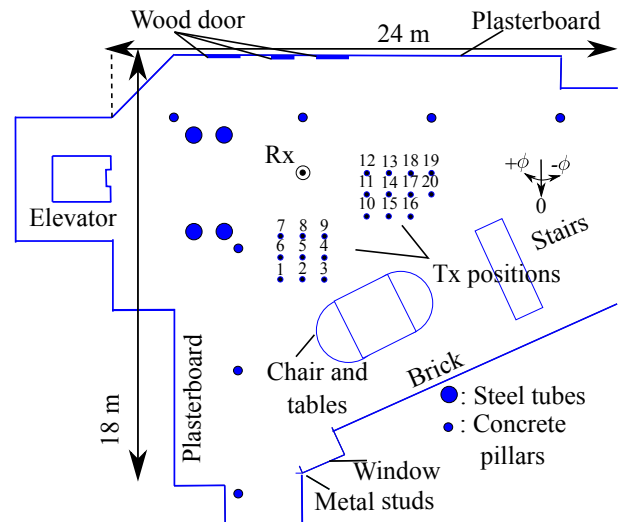| Parameters	Values
Center frequency	28 GHz
Bandwidth	2 GHz
Tx antenna	Commercial biconical antenna (A-INFO SZ-2003000) [31]
Rx antenna	Modified biconical antenna [30]
Number of Rx elements	360
UCA radius	0.24 m
Number of frequency bins	750
Maximum delay	375 ns
Tx and Rx height	1.5 m

Fig. 3: Measurement floor plan in the hall environment [17, 28].
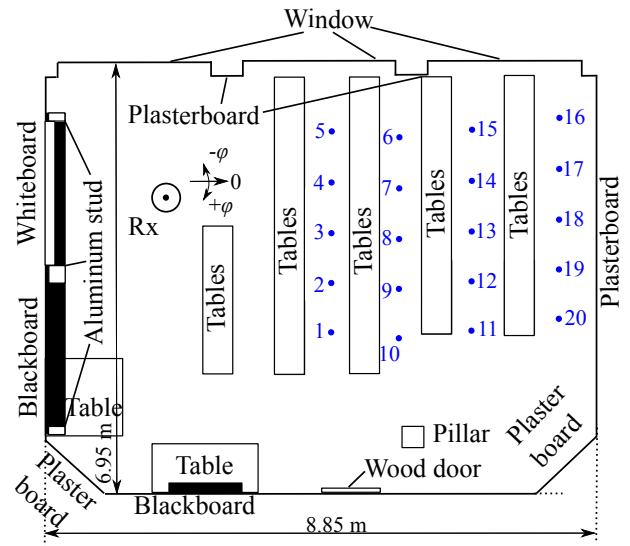

Fig. 4: Measurement floor plan in the classroom environment [7, 29].

MPCs could be clustered properly based on the IO of a group of IOs' locations and the AoA-DT domain with few unidentified clusters. There were some clusters with a mixture of SB and DB MPCs as they had similar AoA and DT and could not be distinguished because of the resolution limit
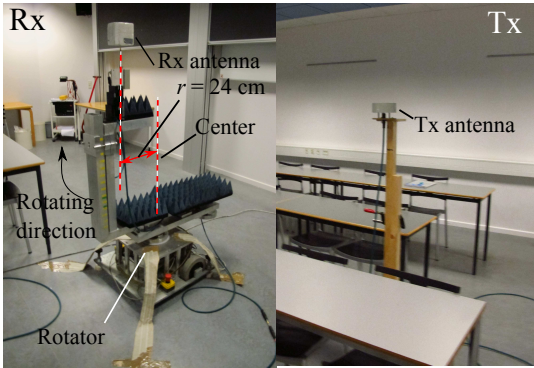
Fig. 5: Photo of the measurement.

of parameter estimation [17]. There were approximately 10 strong clusters in both environments, which interacted from large objects such as pillars, tubes, elevator, brick, plasterboard, windows, and boards. Furthermore, the classroom environment generally had a higher number of strong and higher-order bounce clusters due to a stronger guiding effect of the room. After tracking the clusters, the major 9 SB clusters in hall environment, 6 SB and 5 DB clusters in classroom environment were identified as illustrated in Figs. 8 and 9. These clusters accounted for the majority of the channel power.

4.3 Cluster Spread Results

This section presents the AS and DS mean of major clusters depicted in Figs. 8 and 9. Table 2 illustrates the mean of the major clusters' AS and DS in the hall environment. The last row of Table 2 also shows the mean AS and DS of every cluster. It can be observed that the AS and DS were mostly smaller than 2 deg and 1 ns, respectively. This is because most of these objects had a large and smooth surface in relation to the wavelength and thus the specular components dominated the diffuse components. Tube+pillar, Plasterboard, and Tubes 2 had larger AS and/or DS than other clusters because they comprised of SB or/and DB MPCs scattered from few surfaces located near to each other as depicted in Fig. 8.

Table 2: Cluster AS and DS in hall environment

IO	AS [deg]	DS [ns]
Tubes 1	1.9	1.6
Elevator	1.2	0.4
Brick	0.6	0.3
Metal stud + window	0.8	0.3
Pillar 1	1.3	0
Pillar 2	0	0
Tube+pillar	2.8	0.4
Tubes 2	2.8	2.1
Plasterboard	3.5	0.5
Total	1.7	0.6

Table 3 shows the mean of the major SB and DB clusters' AS and DS in classroom environment. In DB cluster case, the name is given as the Tx side IO followed by Rx side IO. The last row of Table 3 also shows the mean AS and DS of every cluster. Even though the IOs were more complex than those in the hall environment, AS and DS of the majority of clusters were also mostly smaller than 2 deg and 1 ns, indicating the dominance of specular components. However, the clusters with at least one interaction with blackboard and whiteboard (Boards, Front wall-Boards, and Window-Boards + Boards-Window) mostly had larger AS and/or DS than other clusters because the IOs comprised of several flat surfaces with 10-20 cm separation. Furthermore, the mean of all clusters in both hall and classroom environments were approximately the same at 1.7 deg and 0.6 ns. Therefore, the results implied that the channels at 28 GHz were highly directive and the spreads were strongly dependent on the number of surfaces and trajectories of each cluster. Moreover, the overall spreads were similar for both rooms which indicated that they were independent of the environment.

Table 3: Cluster AS and DS in classroom environment

IO	AS [deg]	DS [ns]
Plasterboard	1.9	0.6
Window	1.2	2
Slant left	1.7	0.5
Front wall	1.2	0.2
Slant right	1	0.3
Boards	3.5	0.9
Plasterboard-Window	2	0.7
Window-Front wall	0.4	0.2
Plasterboard-Boards	0.5	0.6
Front wall-Boards	2.3	0.6
Window-Boards + Boards-Window	4.2	1
Total	1.7	0.6

5. Conclusion

In this paper, the geometry-based cluster spread characteristics in hall and classroom environment at 28 GHz were presented. VNA-based channel sounder with the rotator to mimic the UCA system was used to measure the channels. The results implied that there were few strong clusters from large objects in both environments. Furthermore, there were more higher-order bounce clusters in classroom environment due to the guiding effect of a smaller room. The total AS and DS mean in both environments were the same and they were mostly less than 2 deg and 1 ns except the clusters where the MPCs interacted with several surfaces. This indicates that the channels were highly specular at 28 GHz regardless
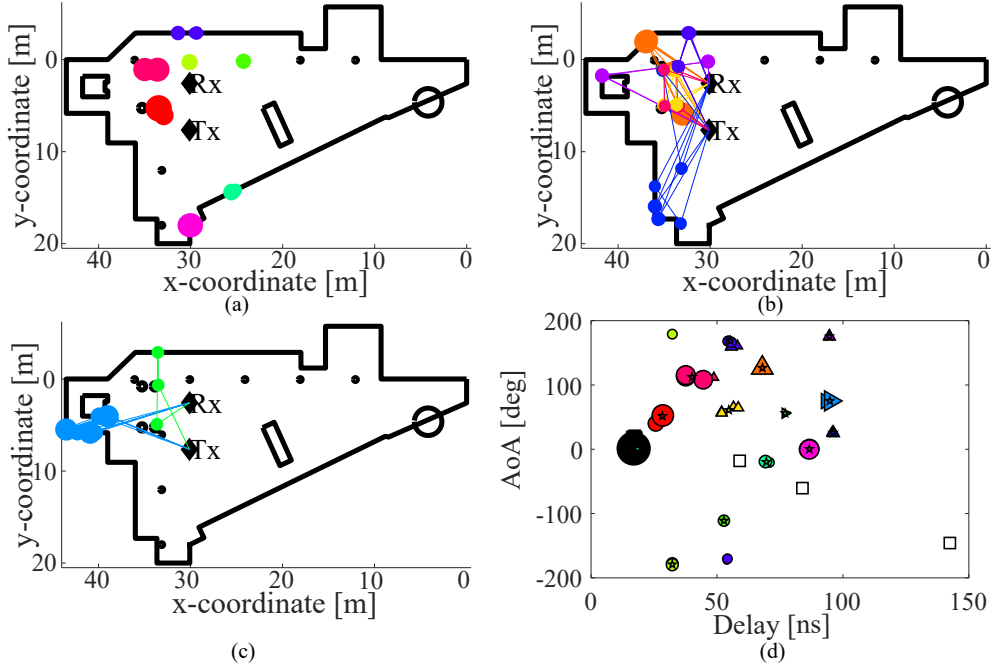
Fig. 6: Clustering results in the hall environment at snapshot 2 ((a) SB, (b) DB, (c) TB, (d) Scatter plot) [17].
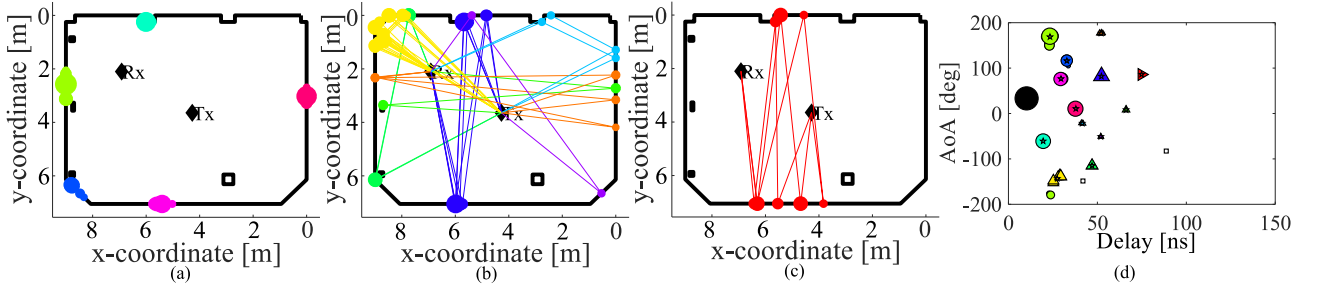

Fig. 7: Clustering results in the classroom environment at snapshot 2 ((a) SB, (b) DB, (c) TB, (d) Scatter plot).
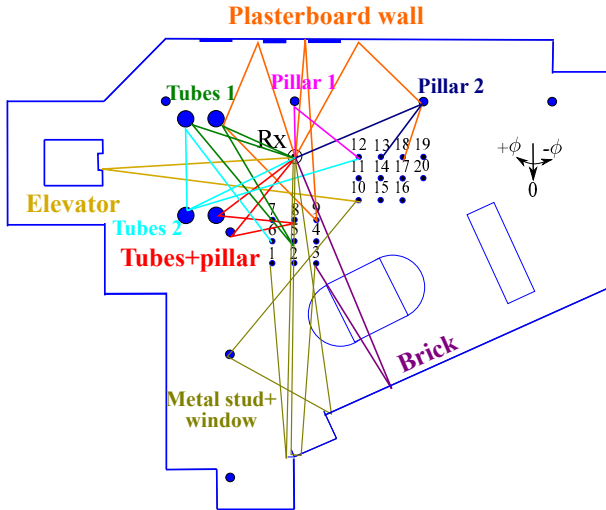

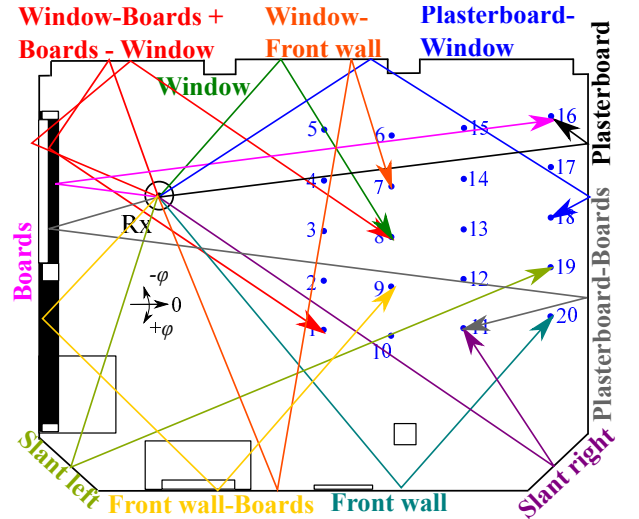Fig. 8: Major clusters in the hall environment [17].

Fig. 9: Major clusters in the classroom environment.

of the environment in consideration. Moreover, the same parameter sets for cluster spreads could be used for the channel model as they are environment independent. As future work, the same analysis steps will be done at different frequencies.

ing setup.

References

[1] K. Sakaguchi *et al.*, "Millimeter-wave wireless LAN and its extension toward 5G heterogeneous networks," *IEICE Trans. on Commun.*, vol. E98-B, no. 10, pp. 1932–1948, July 2015.

[2] T. S. Rappaport *et al.*, "Millimeter wave mobile communications for 5G cellular: It will work!" *IEEE Access*, vol. 1, pp. 335–349, 2013.

[3] G. R. Maccartney, T. S. Rappaport, S. Sun, and S. Deng, "Indoor office wideband millimeter-wave propagation measurements and channel models at 28 and 73 GHz for ultra-dense 5G wireless networks," *IEEE Access*, vol. 3, pp. 2388–2424, 2015.

[4] M. Lei, J. Zhang, T. Lei, and D. Du, "28-GHz indoor channel measurements and analysis of propagation characteristics," in *2014 IEEE 25th Annual International Symposium on Personal, Indoor, and Mobile Radio Communication (PIMRC)*, Sept 2014, pp. 208–212.

[5] X. Wu, Y. Zhang, C. X. Wang, G. Goussetis, H. M. Aggoune, and M. M. Alwakeel, "28 GHz indoor channel measurements and modelling in laboratory environment using directional antennas," in *2015 9th European Conference on Antennas and Propagation (EuCAP)*, May 2015, pp. 1–5.

[6] J. Lee, J. Liang, J. J. Park, and M. D. Kim, "Directional path loss characteristics of large indoor environments with 28 GHz measurements," in *2015 IEEE 26th Annual International Symposium on Personal, Indoor, and Mobile Radio Communications (PIMRC)*, Aug 2015, pp. 2204–2208.

[7] G. Zhang *et al.*, "Experimental characterization of millimeter-wave indoor propagation channels at 28 GHz," *IEEE Access*, vol. 6, pp. 76 516–76 526, 2018.

[8] X. Wu, Y. Zhang, C. X. Wang, G. Goussetis, e. H. M. Aggoune, and M. M. Alwakeel, "28 GHz indoor channel measurements and modelling in laboratory environment using directional antennas," in *2015 9th European Conference on Antennas and Propagation (EuCAP)*, May 2015, pp. 1–5.

[9] M. Peters *et al.*, "Measurement results and final mmMAGIC channel models," May 2017, deliverable D2.2.

[10] R. J. Weiler *et al.*, "Quasi-deterministic millimeter-wave channel models in MiWEBA," *EURASIP J. Wireless Commun. and Networking*, vol. 2016, no. 1, p. 84, Mar 2016.

[11] P. Hanpinitsak, K. Saito, J. Takada, M. Kim, and L. Materum, "Multipath clustering and cluster tracking for geometry-based stochastic channel modeling," *IEEE Transactions on Antennas and Propagation*, vol. 65, no. 11, pp. 6015–6028, Nov 2017.

[12] F. Fuschini *et al.*, "Analysis of in-room mm-wave propagation: Directional channel measurements and ray tracing simulations," *Journal of Infrared, Millimeter, and Terahertz Waves*, vol. 38, no. 6, pp. 727–744, Jun 2017.

[13] S. Kishimoto, M. Kim, D. He, and K. Guan, "Scattering process identification and cluster analysis for millimeter-wave indoor channel model," in *2018 International Symposium on Antennas and Propagation (ISAP)*, Oct 2018, pp. 1–2.

[14] M. Kim, T. Iwata, K. Umeki, J. Takada, and S. Sasaki, "Indoor channel characteristics in atrium entrance hall environment at millimeter-wave band," in *2017 11th European Conference on Antennas and Propagation (EUCAP)*, March 2017, pp. 707–710.

[15] D. Dupleich, F. Fuschini, R. Mueller, E. Vitucci, C. Schneider, V. Degli Esposti, and R. Thomä, "Directional characterization of the 60 ghz indoor-office channel," in *2014 XXXIth URSI General Assembly and Scientific Symposium (URSI GASS)*, Aug. 2014, pp. 1–4.

[16] K. Wangchuk *et al.*, "Double directional millimeter wave propagation channel measurement and polarimetric cluster properties in outdoor urban pico-cell environment," *IEICE Trans. Commun.*, vol. E100-B, no. 7, pp. 1133–1144, Jul 2017.

[17] P. Hanpinitsak, K. Saito, W. Fan, J. Hejselbaek, J. Takada, and G. F. Pedersen, "Frequency characteristics of geometry-based clusters in indoor hall environment at shf bands," *IEEE Access*, 2019.

[18] R. Verdone and A. Zanella, *Pervasive Mobile and Ambient Wireless Communications*. Springer, 2012.

[19] N. Czink, P. Cera, J. Salo, E. Bonek, J. P. Nuutinen, and J. Ylitalo, "A framework for automatic clustering of parametric MIMO channel data including path powers," in *IEEE 64th Vehicular Technology Conference (VTC 2006 Fall)*, Sept 2006, pp. 1–5.

[20] P. Hanpinitsak, K. Saito, J. Takada, M. Kim, and L. Materum, "Clustering method based on scatterer locations for indoor dynamic MIMO channel," in *2016 10th European Conference on Antennas and Propagation (EuCAP)*, April 2016, pp. 1–4.

[21] W. Fan, I. Carton, J. Ø. Nielsen, K. Olesen, and G. F. Pedersen, "Measured wideband characteristics of indoor channels at centimetric and millimetric bands," *EURASIP J. Wireless Commun. and Networking*, vol. 2016, no. 1, p. 58, Feb 2016.

[22] J. Hejselbaek, W. Fan, and G. F. Pedersen, "Ultrawideband VNA based channel sounding system for centimetre and millimetre wave bands," in *Proc. 27th Personal, Indoor, and Mobile Radio Commun. (PIMRC)*, Sept 2016, pp. 1–6.

[23] B. Fleury, M. Tschudin, R. Heddergott, D. Dahlhaus, and K. Ingeman Pedersen, "Channel parameter estimation in mobile radio environments using the SAGE algorithm," *IEEE J. Select. Areas Commun.*, vol. 17, no. 3, pp. 434–450, Mar 1999.

[24] H. V. Pham, M. Kim, and J. Takada, "Cluster-based indoor radio channel characterization at 11GHz," IEICE Technical Report, Tech. Rep. 487, AP2013-200, Mar 2014.

[25] Y. Ji, W. Fan, and G. F. Pedersen, "Channel estimation using spherical-wave model for indoor los and obstructed los scenarios," in *Proc. 11th European Conf. Antennas and Propagation (EUCAP)*, March 2017, pp. 2459–2462.

[26] K. Haneda, J. Takada, and T. Kobayashi, "A parametric UWB propagation channel estimation and its performance validation in an anechoic chamber," *IEEE Trans. Microwave Theory Tech.*, vol. 54, no. 4, pp. 1802–1811, June 2006.

[27] J. Poutanen *et al.*, "Development of measurement-based ray tracer for multi-link double directional propagation parameters," in *Proc. 3rd European Conf. on Antennas and Propagation (EuCAP)*, March 2009, pp. 2622–2626.

[28] G. Zhang *et al.*, "Millimeter-wave channel characterization at large hall scenario in the 10 and 28 GHz bands," in *Submitted to the 13th European Conf. Antennas and Propagation*, March 2019.

[29] P. Hanpinitsak, K. Saito, W. Fan, J. Takada, and G. F. Pedersen, "Frequency characteristics of path loss and delay-angular profile of propagation channels in an indoor room environment in SHF bands," in *IEICE Technical Conf. Short Range Wireless Commun. (TCSRW)*, Mar 2017, pp. 1–6.

[30] S. S. Zhekov, A. Tatomirescu, and G. F. Pedersen, "Modified biconical antenna for ultrawideband applications," in *Proc. 10th European Conf. Antennas and Propagation (EuCAP)*, April 2016, pp. 1–5.

[31] "Sz-2003000," http://www.ainfoinc.com/en/pro_pdf/new_products/antenna/Bi-Conical%20Antenna/tr_SZ-2003000-P.pdf, Ainfoinc, accessed: 2018-11-26.